*Journal of Metallurgy and Materials Science, Vol. 63, No. 3-4, July-December 2021*
*Printed in India, © NML, ISSN 0972-4257*

# Evolution of Nano-crystalline Structures in Aluminium under Rapid Solidification using Molecular Dynamics Simulation

**SUNIL KUMAR*, SUCHANDAN KUMAR DAS, AND SHEULI HORE**
CSIR-National Metallurgical Laboratory, Jamshedpur 831007, INDIA

***Abstract :*** The molecular dynamics (MD) simulation has used to explore the effect of cooling rate on the crystal nucleation and its growth. Themodynamic analysis (potential energy), atomic mean square displacement and diffusion coefficient have considered to characterize the thermal motion of aluminium. The proportions of locally crystal organization such as fcc, bcc, hcp, etc. of aluminium atoms depend on the cooling rate. For cooling rate 0.1K/ps and 1K/ps (cooling from 1173K to 273K), an fcc crystalline solid aluminium is formed during cooling. But for cooling rate 10K/ps, an amorphous aluminium metal is formed at 273K. The dislocation extraction algorithm (DXA), consists of dislocation of the boundary and Burgers vectors have used to characterize the crystal defect in solidification of aluminium. For cooling rate 0.1K/ps, at the stage of nucleation, many crystal defects are found, but as temperature decreases, crystal defect slowly disappears. In case of cooling rate 1K/ps, crystal defects have seen in very early stage of nucleation but these defects grow continuously as temperature decreases. The thermodynamic analysis behind the origin of crystalline and amorphous aluminium has studied. The face center crystal, fcc, structure of aluminium is a most favorable energy state. Amorphous aluminium is an energetically unfavorable metastable state. Diffusion coefficient decrease as the solidification proceeds, but at the nucleation of crystal, it display a sudden decrease to a negative value and then become nearly zero. An abrupt drop to a negative value, comes due to attractive nearest-neighbor lattice packing and crystal nucleation and its growth.

## 1. INTRODUCTION

Under the rapid solidification process (RSP) of metals and alloys, phase transition can be formed depending on the thermal motion of atoms. At extremely high cooling rate, the crystallization may be inhibited and a metallic glass are formed. Under such situations, the liquid phases with the short-range order structures are saved in the solid state [1]. Studying the phase transition phenomena in metallic material at such extremely high cooling rate is not experimentally feasible. The aim of this work should be to study the structural evolutions in aluminum during RSP using MD simulations. The crystallization during RSP needs to be investigated and the effect of crystalline behavior of the re-melting temperature may be investigated if required. From last two decades, scientists have shown that metal processing such as rapid solidification, controls the most micro structural properties of aluminium metal by using both experimental [1-16] and computational simulation[19-35] methodology.

Experimentally, rapid solidification process have carried out by using gas atomization[10], spray atomization [11], melt spinning [12], glass-fluxing method [13], drop tube technique [14], rapid quenching [15], etc. The rapid thermal energy extraction that occurs during rapid cooling create a solid state of material which have large deviations from equilibrium, shows many changes in material properties such as an extension of solid solubility, formation of non-equilibrium or meta-stable crystalline phases, retention of disordered structure, modification of grains shape and size. These properties are responsible for enhancement in mechanical properties, thermal stability, wear resistance, and high temperature strength etc. compared to the conventional solidification process. Recently, Wang *et al.* [16] have shown that the creation of homogeneous microstructures which improve mechanical properties of aluminium alloy by increasing the cooling rate through roll casting technique. Overman *et al.* [17] have studied the microstuctural characteristic and mechanical properties of rapid solidify aluminium alloy both at room temperature and 300K. They have found the ultimate tensile strength 544.2 MPa at room temperature and 298.0 MPa at 300 °C. Despite of many experimental studies, there is a need of study of atomic/molecular modeling of rapid solidification of aluminium at the nanometer scale and cooling rate above $10^7$K/ps, which is more difficult by experiments.

**Corresponding Author :**
Email: sunil@nmlindia.org

Atomic/molecular modeling and mathematical analysis also have used to study the rapid solidification [19-35] by few research groups. They have studied the structural order formation, internal energy evolution, common neighbor analysis, cluster formation during solidification, etc at various cooling rates. However, we also need to study the crystal structure formation, detection of crystal defect, mass diffusion, thermodynamics of cluster formation in rapid cooling process for a complete study of aluminium metal. Some recently published article has explained structure order formation in aluminium metal during rapid cooling process by Hou *et al*.[19]. They have used a wide range of cooling rate ($10^{13}$ to $10^{11}$K/ps) to study the short – range ordered structure in aluminium by using MD simulation. They have found that the cooling rate influence the microstructure only near the liquid–solid transition temperature. They have found mostly two type of structure icosohedral and face centered cubic during fast and slow cooling rate. However, they have not discussed about mass diffusion and the dynamics of the solidification or liquid formation. Some other research groups [20] have also shown that the FCC and metastable HCP structure can co-exist depending on the cooling rate. Liu *et al*. [21] have studied the local atomic structures evolution of aluminium on different cooling rates. They have determined a critical quenching rate at above the glass exhibits the highest structural stability. Further, in literature [54-56], recently classical and reactive molecular dynamics simulation have applied to investigate solidification, mechanical properties and oxidation of aluminium at nano-scale. Despite various studies of structural organization, we also need to study the crystal defect, thermodyanamics of solidification, mass diffusion and the dynamics of solidification at different cooling rate.

Nanoscopic motion of aluminium atoms during solidification, such as self diffusion of atoms in liquid state, or diffusion from liquid to crystal surface is tough to measure experimentally. Though, this motion is one of the most straight forward to visualize by MD. However, apart from visualization, this information does not actually give one much insight into the physics of how and why atoms or molecules move. A more quantifiable measure is essential, of which the self-diffusion coefficient is one of the most common and useful. Hence, we study the short range ordered crystal structure, along with mass diffusion and dynamics during both cooling of aluminium. This study will enhance our understanding on both academic and industrial purposes. We have used large scale MD simulation to study the behavior of aluminium metal during both rapid cooling and rapid heating. For characterization of solidification and melting process behavior, pair distribution function, center of symmetry, bond orientational order and mean square displacement have been computed to elucidate aggregation of atoms, crystal structure formation and solidification dynamics respectively.

## 2. MD SIMULATIONS

For MD simulation, We have used LAMMPS [36], VMD [37] and OVITO [38] softwares for simulation, trejectory visualization and data analysis. The EAM force field as given by Mendelev *et al.* [39] is used here. The total energy, $E$ is given by

$$E = \sum_{i=1}^{N-1} \sum_{j=i+1}^{N} \varphi_{ij}(r_{ij}) + \sum_{i=1}^{N} F_i(\rho_i) \tag{1}$$

$$\rho_i = \sum_{i} \psi(r_{ij}) \tag{2}$$

Where $\psi$ ($r_{ij}$) is the electron density of aluminium atoms. The equation of motion of aluminium atoms can be written as

$$m\frac{d^2 r_i}{dt^2} = F_i = -\nabla_i E \tag{3}$$

The equation (3) is integrated at time step using velocity Verlet algorithm [40] as given in equation (4) and (5).

$$r_i(t+\Delta t) = r_i(t) + v_i(t)\Delta t + \frac{1}{2}(\Delta t)^2 a_i(t+\Delta t) \quad (4)$$

$$v_i(t+\Delta t) = v_i(t) + \frac{1}{2}\Delta t[a_i(t) + a_i(t+\Delta t)] \quad (5)$$

Here *v* and *a* are velocity and acceleration of the $i^{th}$ atom.

For the study of solidification and melting process, we have created a simulation system by placing aluminum atoms with an ideal FCC structure (lattice parameter 4.05Å) in a 3D simulation box with periodic boundary conditions. The MD simulation framework comprises of two steps: first is equilibration and second is cooling process. In equilibration, the temperature of system is maintained at 1173 and 273K for solidification and melting process respectively, for 100ps to attain an energetically favorable liquid state.

The temperature of system decrease from 1173 to 273K for solidification by using a wide range of cooling rate such as 10 K/ps, 5K/ps, 4K/ps, 2K/ps, 1K/ps, 0.5K/ps, 0.4K/ps, 0.2 K/ps and 0.1K/ps. The pressure of simulation system is maintained at 0bar for equilibration and solidification and melting step. All these temperature and pressure parameters are controlled by Nose-Hoover thermostat and Andersen barostat which is available in open source LAMMPS. The density and internal energy at liquid and solid state have calculated which are found to similar to experimental or simulation published results as given in ref [19]. We stored simulation data at regular interval during simulation for the visualization and analysis.

## 3. RESULTS AND DISCUSSIONS

We have discussed our results in the next three sections. In the first section, the study of evolution of various crystal structure during the cooling process, in the second section, the thermodynamics behind the various crystal structure and in the third section shows crystal defects.

### 3.1. *Evolution of crystal nucleation and growth*

The formation of amorphous or crystalline structure in an aluminium sample is expected to depend on the cooling rate. To understand the morphology of the aluminium, the cooling rates have chosen from 0.1K/ps to 10Kps as given in table 1. It is found that three different types of crystal structure have found during cooling: face centered crystal (fcc), hexagonal close packing (hcp) and amorphous depending on cooling rate as shown in figure 1.The initial state of all systems was at liquid state at temperature T=1173K (melting temperature of aluminium $T_m$ =940K). In liquid state all aluminium samples show amorphous structure as given in figure 1 by white atoms. In case of cooling rate 10K/ps, aluminium atoms unable to organize in crystal structure due to very rapid cooling. The atoms are kinetically traps in meta-stable state and unable to form any crystal structure. However, in case of 5K/ps, 1K/ps and 0.1K/ps aluminium atoms are able to form a crystal structure which also strongly depends on the cooling rate. In cooling rate 5K/ps, few small ordered clusters formed, but unable to grow. The ordered cluster has FCC and hcp type crystal structure, but the majority of atoms is organized in random. In case of cooling rate 1K/ps and 0.1K/ps, most of the aluminium atoms are able to crystallize in fcc structure because slowly cooling allow atoms to search most favorable minimum energy state. However, some crystal defect also has seen in the form of amorphous, hcp and other type of packing of atoms. Section 3, consist the detail study of crystal defects.

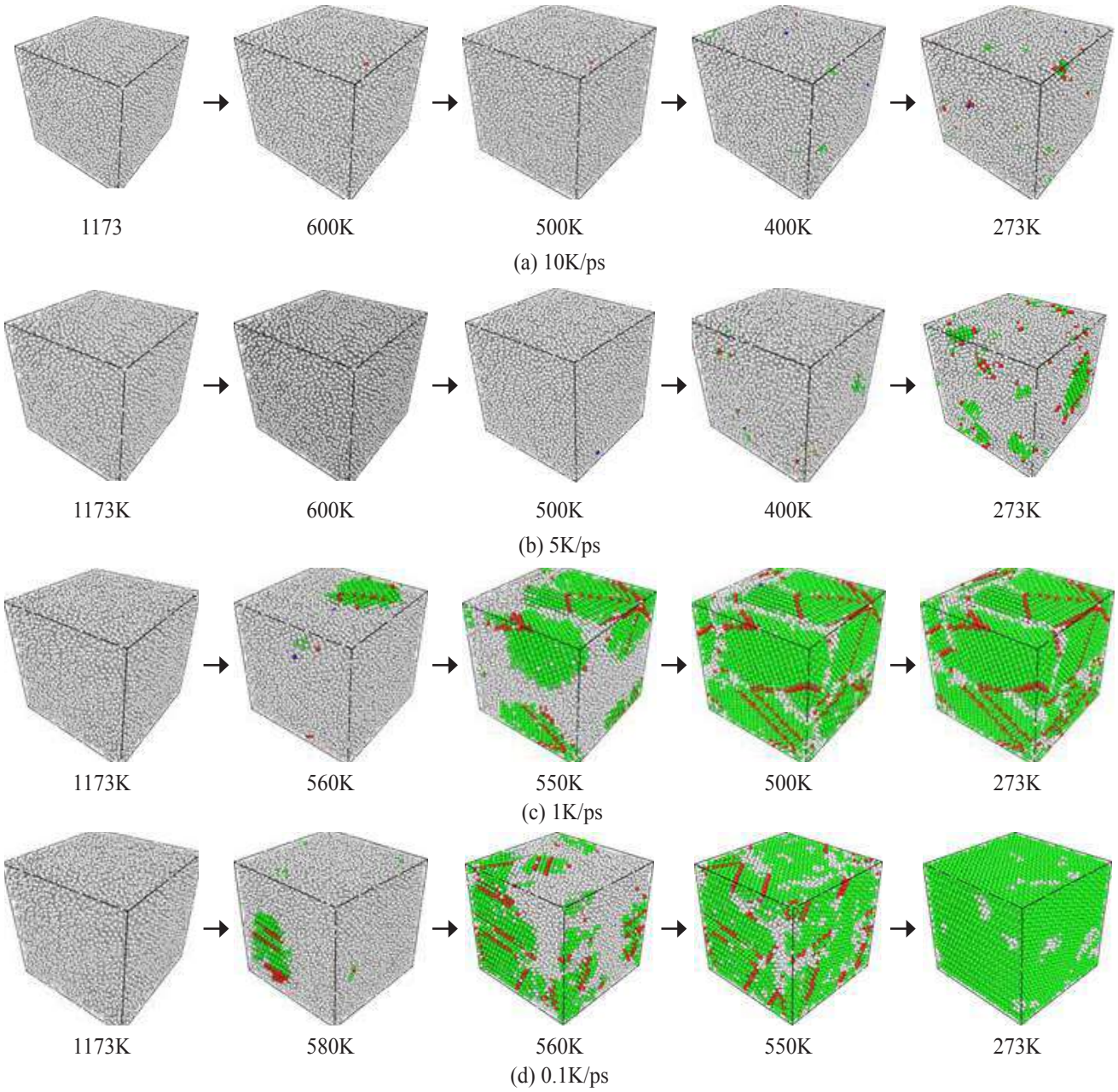


Figure 1. Snapshots of solidification structures under the different cooling rates (a) 10K/ps, (b) 5K/ps, (c) 12K/ps and (d) 0.1K/ps. White, red, blue, and green atoms corresponds to amorphous, HCP, BCC and FCC respectively.

***Table 1 Bond order parameters (BOP) for face-centered-cubic, hexagonal close-packed, simple cubic, body-centered-cubic, liquid [45].***

| Geometry | Q4 | Q6 | W4 | W6 |
|---|---|---|---|---|
| fcc | 0.19094 | 0.57452 | -0.15932 | -0.01316 |
| hcp | 0.09722 | 0.48476 | 0.13410 | -0.01244 |
| sc | 0.76376 | 0.35355 | 0.15932 | 0.01316 |
| bcc | 0.08202 | 0.50083 | 0.15932 | 0.01316 |
| liquid | 0 | 0 | 0 | 0 |

The variables of r- g(r) plots with temperature for three different cooling rates are shown in Figure 2. In case of very rapid cooling 10K/ps, r-g(r) plot shows a sharp peak at around at r = 2.65Å, as the temperature rapidly decreases, the height of peak increase, which corresponds to the aggregation of atoms during the solidification process as shown in figure 2(a). In case of cooling rate 1K/ps and 0.1K/ps, g(r) plot shows a sharp peak at high temperature, but as temperature decreases, peaks at r > 3.00 split in many distinct peaks which indicates that the aluminium atom form long rang ordered structure as shown in figure 2 (b) and (c). Figure 2 (d) shows the radial distribution of aluminium structure at 273K, which have formed through various cooling rates. In all samples, the first peak of gI found at r=2.65Å, but the height of the peak is increased as cooling rate decrease, this shows that low cooling results very close packing of aluminium atoms. However, the other peaks at r > 2.65Å, splits in multiple distinct peaks as cooling rate decreases. These distinct peaks indicating toward evolution of long range ordered packing of aluminium atoms.

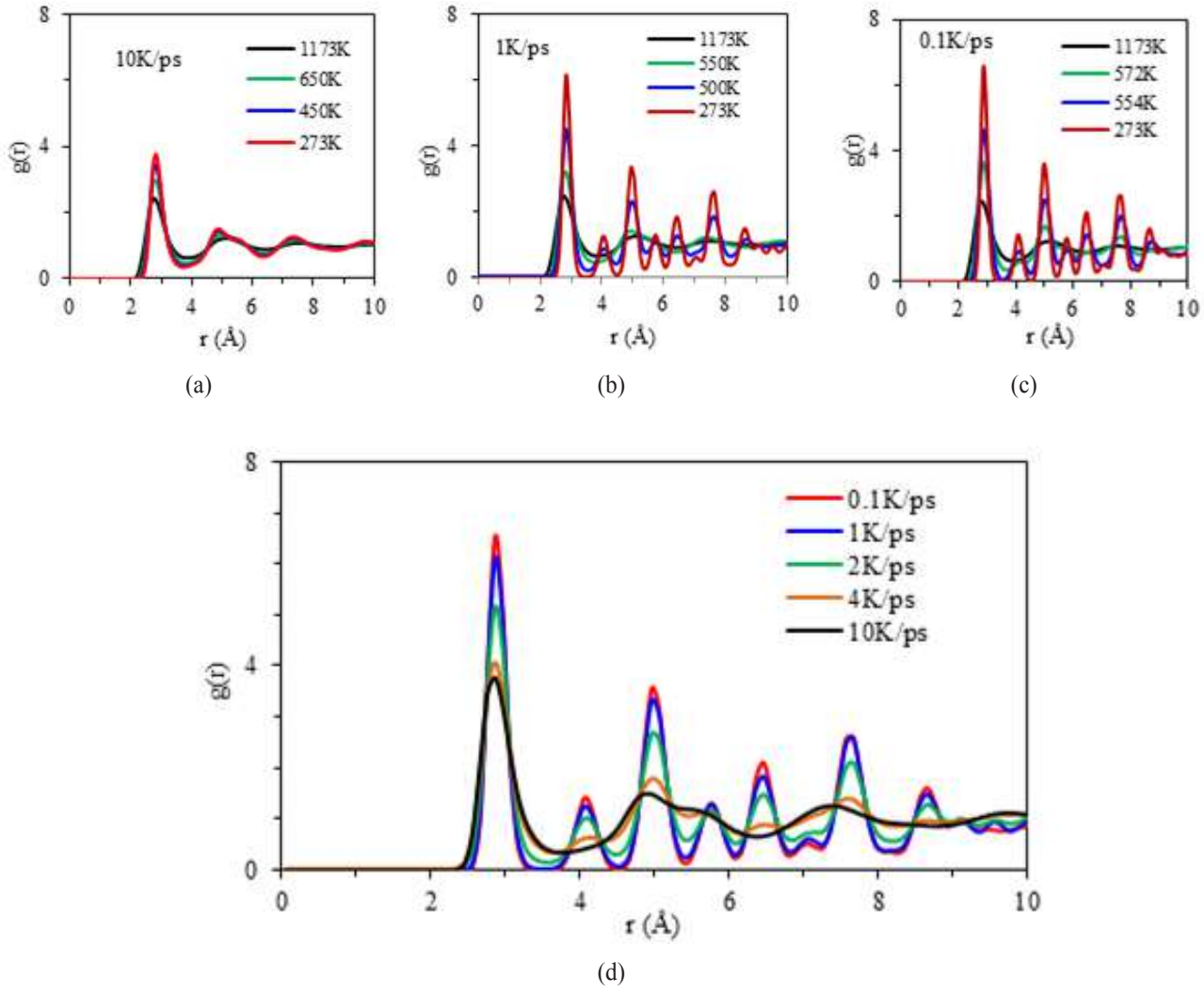


***Figure 2 Variation in g(r) of atoms during various cooling rates: (a) 10K/ps (b) 1K/ps, (c) 0.1K/ps and (d) at 273 K.***

To investigate the growth of crystals, the number or atoms belong to the FCC, hcp, bcc, ico and amorphous have calculated during solidification. The amorphous and crystalline region has separated by using an interface mesh as shown in figure 3. At very early stage of crystal nucleation, a small size cluster of atoms has seen, but as the temperature decreases cluster size increases as given in the snapshot. The packing of atoms in the crystal has found different such as fcc, hcp, bcc and ico depending of cooling rate.

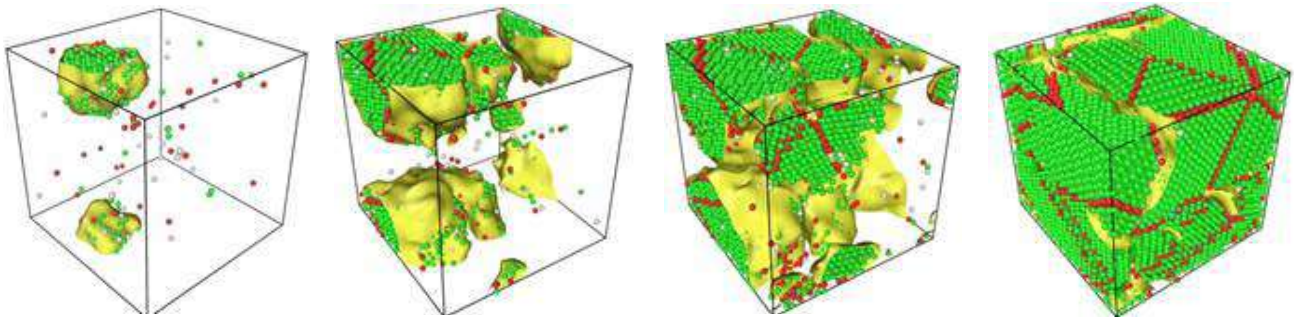

560K (a) 550K (b) 500K (c) 273K (d)

Figure 3 Snapshot of crystal growth during solidification of aluminium at cooling rate 1K/ps. For clear visualization only cluster of crystalline atoms has shown and free region belongs to amorphous atoms. White, red, blue, and green atoms correspond to amorphous, HCP, BCC and FCC respectively.

Figure 4 shows the number of atoms belongs to fcc, hcp, bcc, ico and amorphous have calculated as temperature decreases. In case of cooling rate, 0.1 K/ps, an instant growth of nucleation have found at around 570 to 550K. The number of atoms belongs to fcc crystal increases very rapidly and simultaneously amorphous atoms decreases, which indicates that crystal nucleation and growth occurs at around 570 to 550K. However, atom belongs in bcc, hcp, and ico an appearing during nucleation but as the crystal grows, these atoms have disappeared. But, in case of cooling rate, 1K/ps, gradual growth of crystal have found at around temperature, 530 to 480 K. The atoms belong in fcc and hcp increases gradually as temperature decreases, simultaneously amorphous atom gradually decreases. In case of very rapid cooling rate, 10K/ps, atoms belong to fcc, bcc, hcp and ico are very minor and fluctuate near zero as shown in figure 4c.

(a) 0.1K/ps

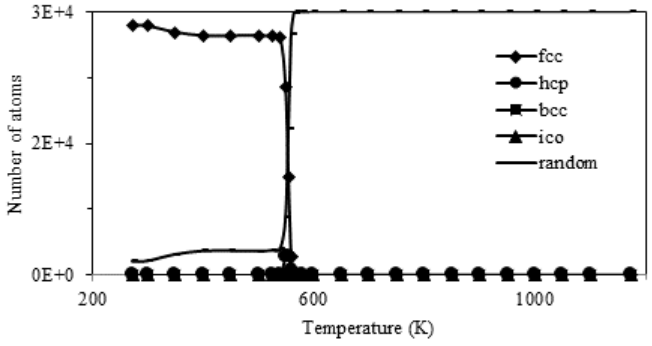


(b) 1K/ps

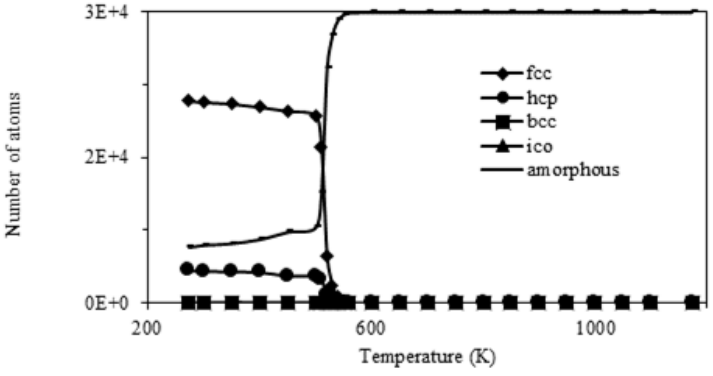

(c) 10K/ps

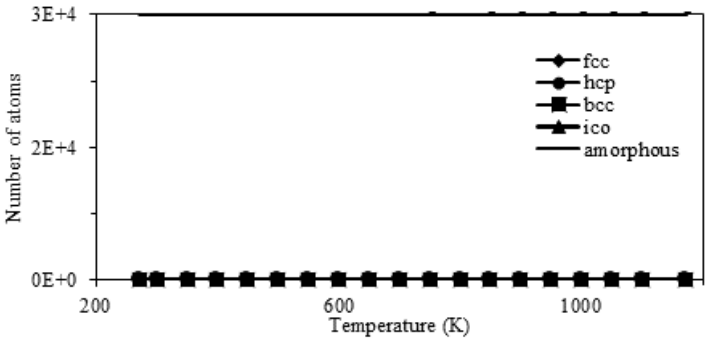


***Figure 4 number of atoms belong to different crystal packing are plotted during cooling at various cooling rates: (a) 0.1K/ps, (b) 1K/ps and (c) 10K/ps.***

### *Global bond order parameter*

The bond-orientational order parameters *Q*4, *Q*6, *W*4, and *W*6, used to characterize the crystalinity of aluminium by quantitatively during rapid solidification of aluminium as given in figure 5. The numerical value of *Q*4, *Q*6, *W*4, and *W*6 at temperature 273K and cooling rate 0.1K/ps from our simulations are consistent with the standard values as given in table II. Figure 5 shows the variation of *Q*4 and *Q*6 during solidification at various cooling rates. The numerical values of *Q*4 and *Q*6 remain roughly constant at around zero during cooling from 1173K to nearly 580K. Further cooling, results sharp increament in numerical value of *Q*4 and *Q*6 for cooling rate 0.1 and 1K/ps indicate that atoms organization changes from amorphous to crystalline. In case of cooling rate 10K/ps, the value of both *Q*4 and *Q*6 remains constant near zero throughout the cooling process due to the metastable amorphous organization. Thus the bond-orientational order parameters give a good signature of the melting transition.

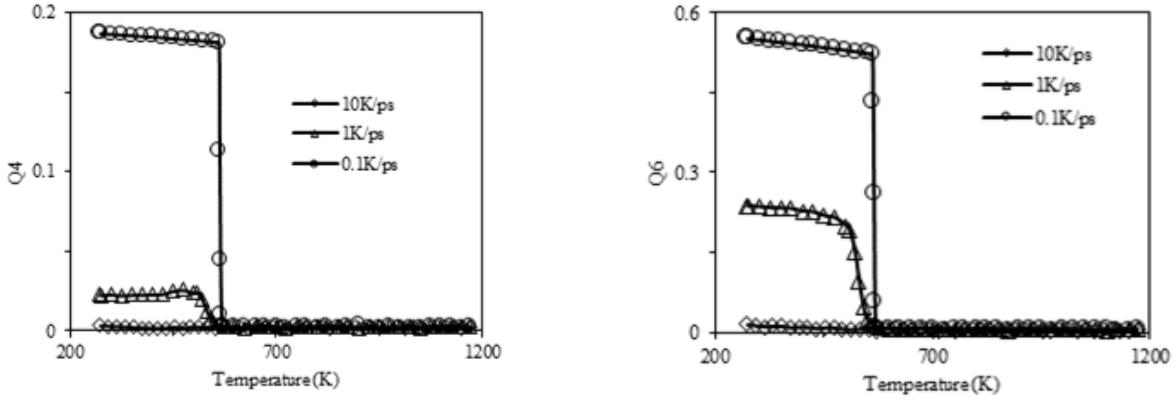


***Figure 5 The variation of bond-orientation order parameters during solidification of aluminum at different cooling rate (a) Q4 and (b) Q6.***

### *Crystal defect*

The dislocation extraction algorithm (DXA) [50-52] has used to characterize the crystal defect in atomic simulations. It can identify crystal defects by continuous lines and determines their Burgers vectors. As the first step of this method, the crystal defect regions are characterized through the common neighbor analysis (I) method. By this method, an interface mesh is built which distinguishes the crystalline atoms from the disordered ones as shown in figure 6. On this interface mesh, a Burgers circuit is constructed for each defect. In case for high cooling rate, 10K/ps, aluminium structure do not form a crystal structure as given in figure 1. For cooling rate 0.1K/ps, at the stage of nucleation, many crystal defects are found but as simulation proceeds and temperature decreases, crystal defect slowly disappears as shown in figure 6 (a). In case of cooling rate 1K/ps, crystal defects have seen in very early stage of nucleation but these defects grow continuously as temperature decreases as shown in figure 6 b.

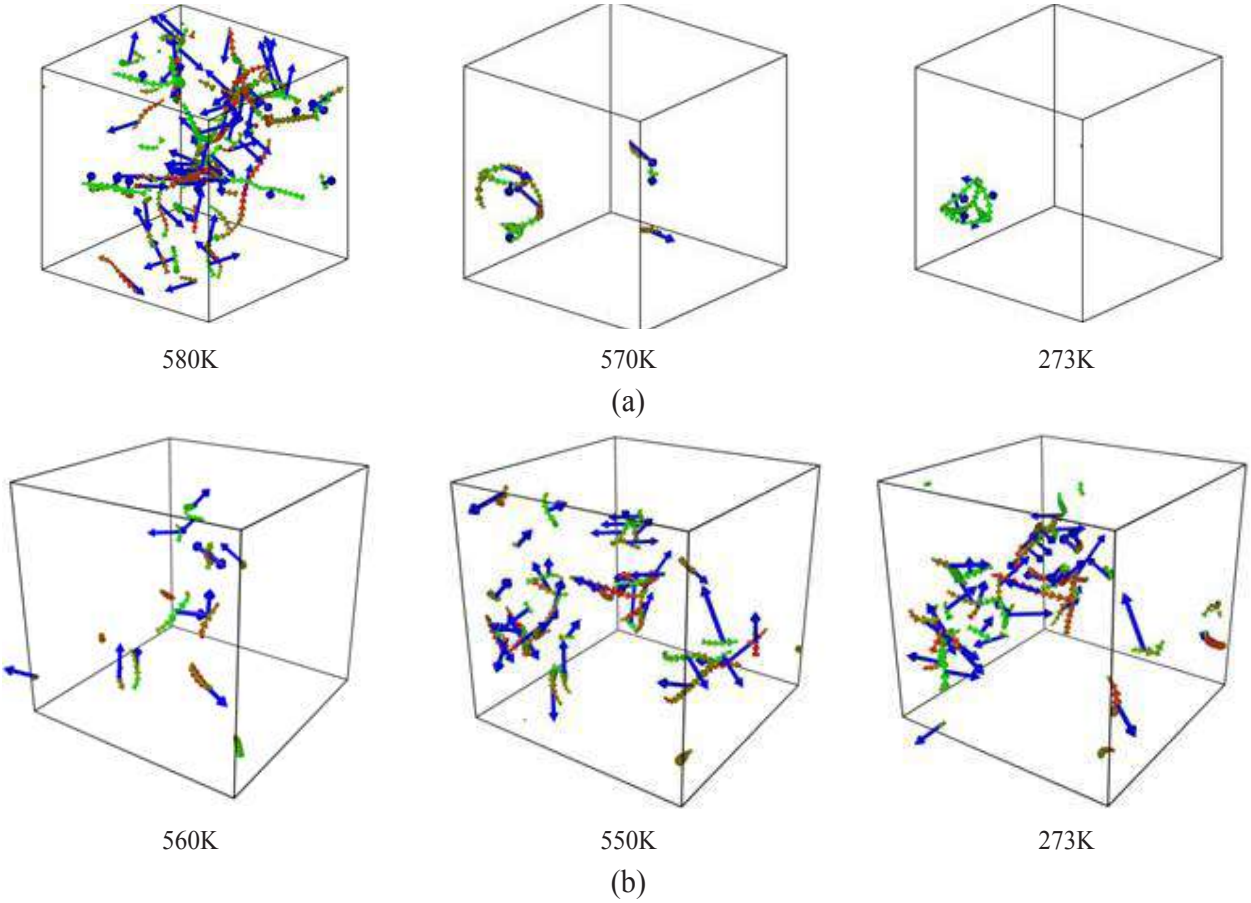


Figure 6 Detection of crystal defect by burger vector during solidification from 1173K to 273K at a different cooling rate: (a) 0.1K/ps and (b) 1K/ps. Screw and edge dislocation are indicated by red and green colors respectively. Blue arrow indicates the burger vector and it is perpendicular to dislocation.

### 3.2. *Thermodynamic analysis of crystal formation during solidification*

Cooling rate controls the mobility and thermal vibrations of aluminium metal which facilitate close packing of atoms and create clusters of atoms with the low energy region as shown in figure 7. The low energy region act as nuclei for crystal growth. As temperature decreases these nuclei grow rapidly and form a long range ordered structures. In figure 7, low and high potential energy atoms are shown in dark red and blue spheres respectively. At high temperature 1173 to 580, the aluminium atoms are in amorphous state with high potential energy as indicated by blue spheres, but as the system further cools, atoms looses potential energy as indicated by red spheres. The aggregation of low energy spheres creates a nucleation region and its growth leads to the formation of long range ordered structure.

The formation and growth of nucleation region, strongly depends on the cooling rate. The snapshot of the potential energy distribution of various cooling rates is shown in figure 7 (a-d). In case of high cooling rate 10K/ps and 5K/ps, a large number of aluminium atoms reached in a low energy state as shown in randomly distributed dark red colored spheres in figure 7 (a) and (b). However, due to very rapid cooling, the atoms are kinetically traps in meta-stable state and unable to form any cluster for crystal nucleation. In case of high cooling rate 1K/ps and 0.1K/ps, a large number of aluminium atoms reached in a low energy state and subsequently aggregates and form a cluster of atoms which act as crystal nucleation as shown in figure 7 (c) and (d). As the system temperature goes down, size of cluster grow very rapidly and form a long range ordered structures.

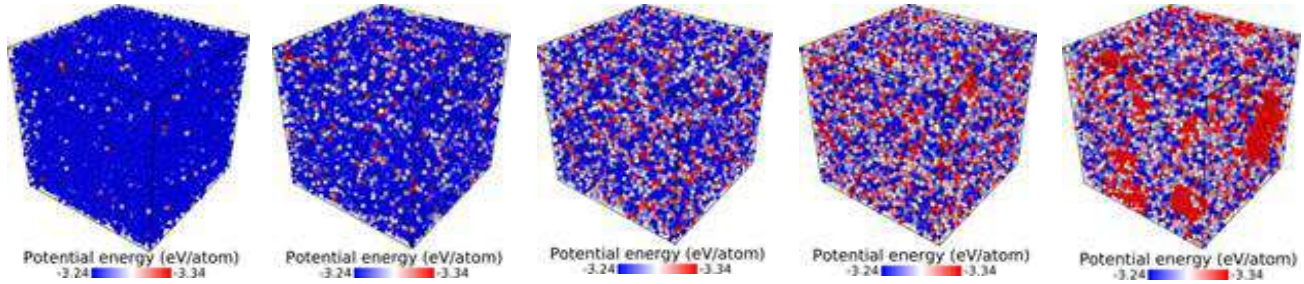


1173 600K 500K 400K 273K

(a) 10K/ps

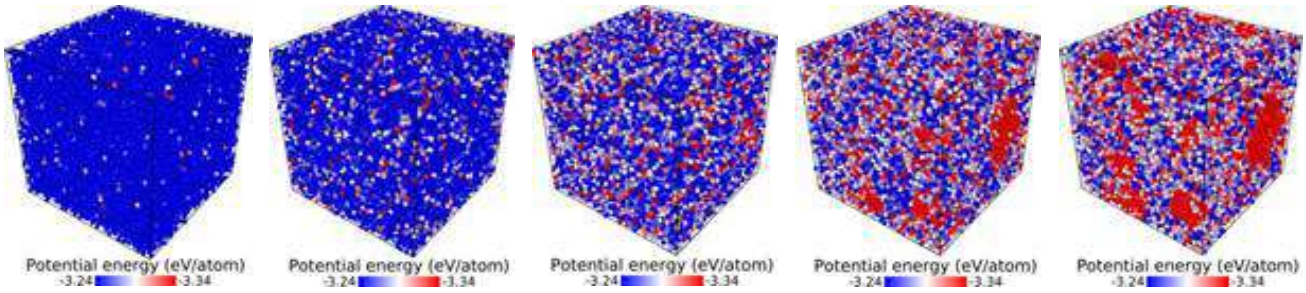


1173K 600K 500K 400K 273K

(b) 5K/ps

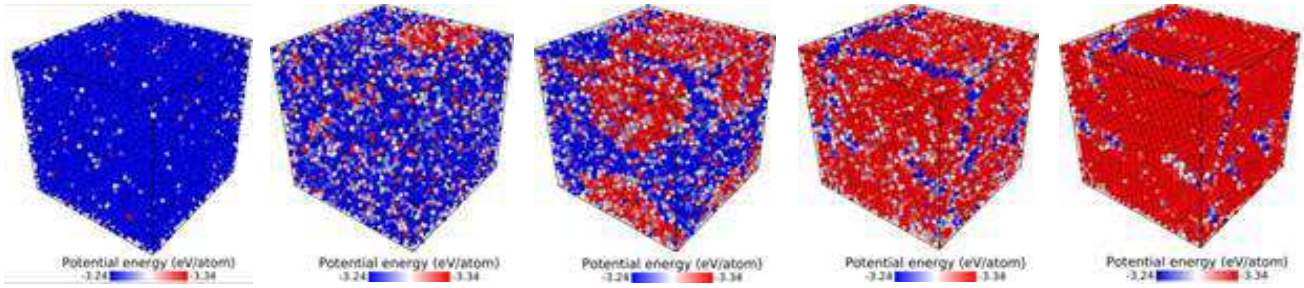


1173K 560K 550K 500K 273K

(c) 1kps

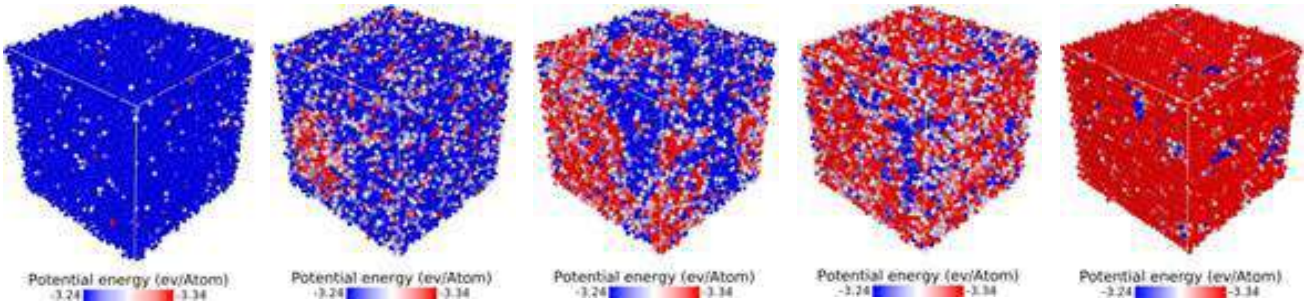


1173K 580K 560K 550K 273K

(d) 0.1K/ps

***Figure 7 Potential energy evolution of each atom at various cooling rates (a) 10K/ps, (b) 5K/ps, (c) 1K/ps and (d) 0.1K/ps,***

***Average energy***

Figure 8 and 9 shows the effect of cooling rate on the potential energy per atom during the solidification process of aluminium. The potential energy of aluminium linearly decreases with the decrease in temperature for the amorphous state for highest cooling 10K/ps. Meanwhile, potential energy of aluminium atoms for slower cooling rate, gradually deviate from the linear relationship with temperature at around 650K due to crystal nucleation and growth at cooling rate < 5K/ps. The temperature of nucleation and its growth where the potential energy begins to sharply decrease, increases with the decrease in the cooling rate. The effect of cooling rate on the energy curve appears only after the nucleation of crystal. At 273K, the energies of solidification of aluminium at different cooling rates do not reach the same value. The low potential energy of aluminium atom found at a very slow cooling rate.

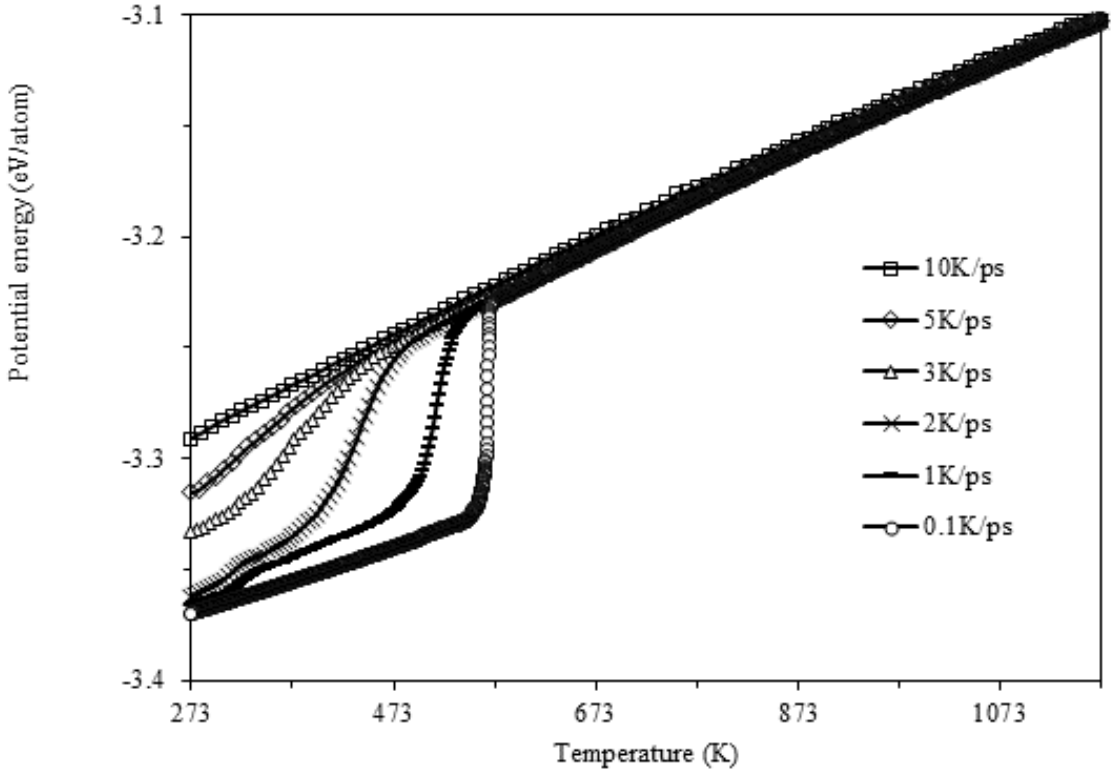


***Figure 8 Effect of temperature on the potential energy of aluminium atoms during solidification at various cooling rates.***

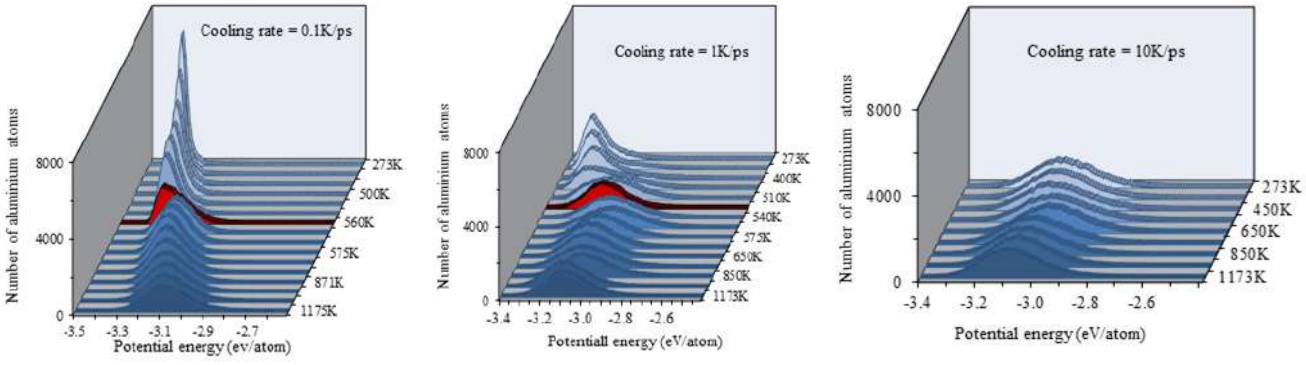


(a) (b) (c)

***Figure 9 Potential energy distribution of aluminium atoms during solidification at various cooling rates: (a) 0.1K/ps, (b) 1K/ps and (c) 0.1K/ps. Red colored histogram indicates the early stage of nucleation during crystal growth.***

### *3.3. Dynamics of solidification process*

The dynamics of the system has been studied using mean square displacement (MSD) of the aluminum atoms is shown in Figure 10. The MSD at a cooling rate of 0.1K/ps is expressively higher than the MSD at a cooling rate of 1 and 10K/ps, indicating the thermal motion and rearrangements of the atoms is higher at the lower cooling rates. It is also showing that high thermal motion and rearrangement facilitate crystal nucleation and growth. In contrast, at the comparatively high cooling rates, i.e. 10 K/ps, a metallic glass structure formed due to the less thermal motion and rearrangement of atoms. Nano-scopic motion of aluminium atoms during solidification, such as self diffusion of atoms in liquid state, or diffusion from liquid to crystal surface is quantitavely evaluated through diffusion coefficient. The numerical value of diffusion coefficient of our simulations is found nearly similar to reported experimental data [53] as given in table 2.

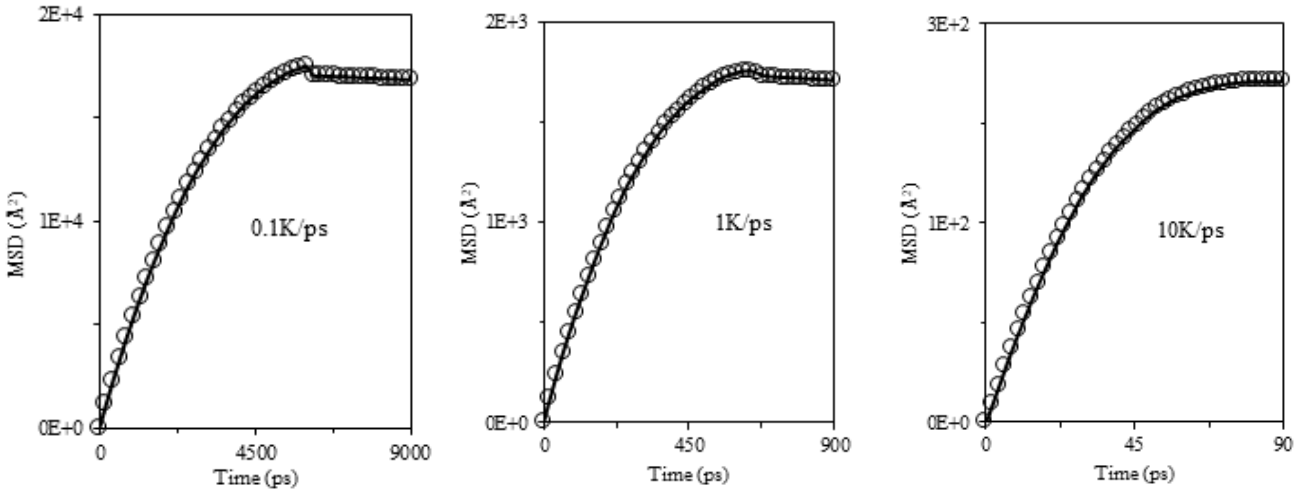


(a) (b) (c)

***Figure 10 Mean square displacement of aluminium atoms during solidification at various cooling rates: (a)0.1K/ps, (b) 1K/ps and (c) 10K/ps.***

Figure 11 (a-c) shows, the time dependent diffusion coefficient aluminium at different cooling rate. At cooling rate 0.1K/ps, diffusion coefficient decrease as the simulation time increases due to solidification of aluminium atoms, but at the nucleation of crystal it shows sudden drop and then become nearly zero. Sudden drop to a negative value, comes due to attractive nearest-neighbor lattice packing at crystal nucleation and growth. In general, the negative diffusion coefficient is showing the process of increasing concentration or cluster formation as opposed to diffusion. In case of very rapid cooling, the diffusion coefficient gradually decreases as the simulation time increases during solidification which indicates that thermal motion of aluminium atoms slowly decreases and does not involve any structural changes.

Figure 11 (d) shows, the variation of the diffusion coefficient with temperatures during the solidification process at various cooling rates. The plot is indicating that the diffusion coefficient strongly depends on the cooling rate. It is gradually decreasing as temperature decreases for very rapid cooling rate, 10K/ps and not seen any abrupt change. But, in case of 0.1 and 1K/ps, it decreases during cooling and shows a sudden dip at around 550K (for 0.1K/ps) and 510K/ps (for 1 K/ps) due to crystal nucleation.

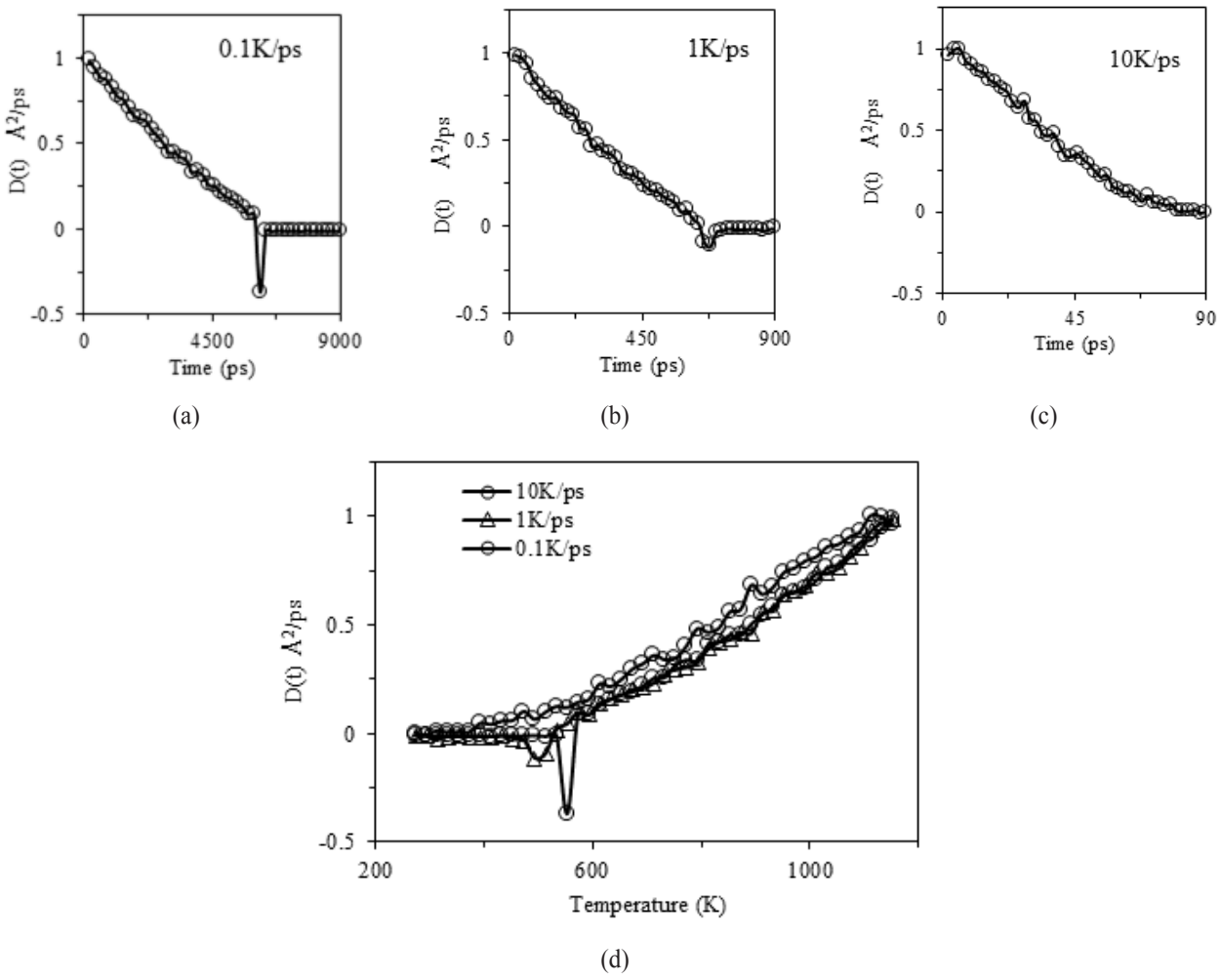


Figure 11 Diffusion coefficient of aluminium atoms during solidification at various cooling rates: (a) 0.1K/ps, (b) 1K/ps and (c) 10K/ps and (d) diffusion coefficients vs temperature plot at different cooling rate.

Table 2. Aluminium self-diffusion coefficients measured by MD simulation at cooling rate 0.1K/ps and its comparison with reported experimental data[53].

| Temperature (K) | From our MD simulation (cooling rate = 0.1K/ps) ($10^{-9}m^2s^{-1}$) | Reported experimental data ($10^{-9}m^2s^{-1}$) |
|---|---|---|
| 980 | 6.45 | 7.2 ± 0.6 |
| 1020 | 7.03 | 7.9 ± 0.7 |
| 1060 | 7.76 | 8.8 ± 0.7 |

## 4. CONCLUSION

The MD simulation method has used to explore the effect of cooling rate on the crystal nucleation and its growth. Themodynamic analysis, MSD and diffusion coefficient have used to describe the thermal motion of aluminium. The proportions of locally ordered organization such as fcc, bcc, hcp, etc. of aluminium atoms depend on the cooling rate. For cooling rate 0.1K/ps and 1K/ps (cooling from 1173K to 273K), an fcc crystalline solid aluminium

is formed during cooling. But for cooling rate 10K/ps, an amorphous aluminium metal is formed at 273K. The dislocation extraction algorithm (DXA), consists of dislocation of the boundary and Burgers vectors have used to characterize the crystal defect in solidification of aluminium. For cooling rate 0.1K/ps, at the stage of nucleation, many crystal defects are found, but as temperature decreases, crystal defect slowly disappears. In case of cooling rate 1K/ps, crystal defects have seen in very early stage of nucleation but these defects grow continuously as temperature decreases. The thermodynamic analysis behind the origin of crystalline and amorphous aluminium has studied. The face center crystal, fcc, structure of aluminium is a most favorable energy state. Amorphous aluminium is an energetically unfavorable metastable state. Diffusion coefficient decrease as the solidification proceeds, but at the nucleation of crystal, it shows a sudden drop to a negative value and then become nearly zero. Sudden drop to a negative value, comes due to attractive nearest-neighbor lattice packing and crystal nucleation and its growth.

## REFERENCE

[1] Y. Birol, Microstructural evolution during annealing of a rapidly solidified Al–12Si alloy. Journal of alloys and compounds 439, 1, 81-86, 2007.

[2] M. Rajabi, M. Vahidi, A. Simchi and P. Davami. Effect of rapid solidification on the microstructure and mechanical properties of hot-pressed Al–20Si–5Fe alloys. Materials Characterization 60, 11, 1370-1381, 2009.

[3] L. Katgerman and F. Dom. Rapidly solidified aluminium alloys by meltspinning. Materials Science and Engineering: A 375, 1212-1216, 2004.

[4] E. Karaköse and M. Keskin. Effect of solidification rate on the microstructure and microhardness of a melt-spun Al–8Si–1Sb alloy. Journal of Alloys and Compounds 479, 1, 230-236, 2009.

[5] O. Uzun, T. Karaaslan, M. Gogebakan and M. Keskin. Hardness and microstructural characteristics of rapidly solidified Al–8–16 wt.% Si alloys. Journal of alloys and compounds 376, 1, 149-157, 2004.

[6] C. L. Xu, H. Y. Wang, F Qiu, Y. F. Yang and Q. C. Jiang. Cooling rate and microstructure of rapidly solidified Al–20wt.% Si alloy. Materials Science and Engineering: A 417, 1, 275-280, 2006.

[7] P. Li, V. I. Nikitin, E. G. Kandalova, and K. V. Nikitin. Effect of melt overheating, cooling and solidification rates on Al–16wt.% Si alloy structure. Materials Science and Engineering: A 332, 1, 371-374, 2002.

[8] C. L. Xu and Q. C. Jiang. Morphologies of primary silicon in hypereutectic Al–Si alloys with melt overheating temperature and cooling rate. Materials Science and Engineering: A 437, 2, 451-455, 2006.

[9] S. P. Nikanorov, M. P. Volkov, V. N. Gurin, Yu A. Burenkov, L. I. Derkachenko, B. K. Kardashev, L. L. Regel and W. R. Wilcox. Structural and mechanical properties of Al–Si alloys obtained by fast cooling of a levitated melt. Materials Science and Engineering: A 390, 1, 63-69, 2005.

[10] G. Antipas, Gas Atomization of Aluminium Melts: Comparison of Analytical Models. Metals 2, 2, 202-210, 2012.

[11] M. Gupta, F. Mohamed and E. Lavernia. The Effect of ceramic reinforcements during spray atomization and codeposition of metal matrix composites: part i. heat transfer. Metallurgical Transactions A 23, 3, 831-843, 1992.

[12] F. T. Wallenberger, N. E. Weston, K. Motzfeldt, and D. G. Swartzfager. Inviscid melt spinning of alumina fibers: chemical jet stabilization. Journal of the American Ceramic Society 75, 3, 629-636, 1992.

[13] M. L. Froberg, Method for preparing molten glass. U.S. Patent 4, 358, 304, issued November 9, 1982.

[14] M. Barth, B. Wei, D. M. Herlach and B. Feuerbacher. Rapid solidification of undercooled nickel-aluminium melts. Materials Science and Engineering: A 178, 1-2, 305-307, 1994.

[15] H. Jones, and C. Suryanarayana. Rapid quenching from the melt: An annotated bibliography 1958–72. Journal of Materials Science 8, 5, 705-753, 1973.

[16] H. Wang, L. Zhou, Y. Zhang, Y. Cai, and J. Zhang. Effects of twin-roll casting process parameters on the microstructure and sheet metal forming behavior of 7050 aluminum alloy. Journal of Materials Processing Technology 233, 186-191, 2016.

[17] N. R. Overman, S. N. Mathaudhu, J. –P. Choi, T. J. Roosendaal, and S. Pitman. Microstructure and mechanical properties of a novel rapidly solidified, high-temperature Al-alloy. Materials Characterization 112, 142-148, 2016.

[19] Z.-Y. Hou, K. Dong, Z. Tian, R. Liu, Z. Wang, and J. Wang. Cooling rate dependence of solidification for liquid aluminium: A large-scale molecular dynamics simulation study. Physical Chemistry Chemical Physics 18, 17461, 2016.

[20] D. M. Herlach, and B. Feuerbacher. Non-equilibrium solidification of undercooled metallic melts. Advances in Space Research 11, 7, 255-262, 1991.

[21] D. Turnbull, Under what conditions can a glass be formed? Contemporary physics 10, 5, 473-488, 1969.

[22] J. Lu and J. A. Szpunar. Molecular-dynamics simulation of rapid solidification of aluminum. Acta metallurgica et materialia 41, 8, 2291-2295, 1993.

[23] C. Kuiying, L. Hongbo, L. Xiaoping, H. Qiyong and H. Zhuangqi. Molecular dynamics simulation of local structure of aluminium and copper in supercooled liquid and solid state by using EAM. Journal of Physics: Condensed Matter 7, 12, 2379, 1995.

[24] C. –S. Liu, Z. –G. Zhu, J. –C. Xia and D.-Y. Sun. Different Cooling Rate Dependences of Different Microstructure Units in Aluminium Glass by Molecular Dynamics Simulation. Chinese Physics Letters 17, 1, 34, 2000.

[25] C. S. Liu, Z. G. Zhu, J. Xia and D. Y. Sun. Cooling rate dependence of structural properties of aluminium during rapid solidification. Journal of Physics: Condensed Matter 13, 9, 1873, 2001.

[26] J. R. Morris, C. Z. Wang, K. M. Ho, and C. T. Chan. Melting line of aluminum from simulations of coexisting phases. Physical Review B 49, 5, 3109, 1994.

[27] A. Sarkar, P. Barat and P. Mukherjee. Molecular dynamics simulation of rapid solidification of aluminum under pressure. International Journal of Modern Physics B 22, 17, 2781-2785, 2008.

[28] S. Solhjoo, A. Simchi and H. Aashuri. Molecular dynamics simulation of melting, solidification and remelting processes of aluminum. Iranian Journal of Science and Technology. Transactions of Mechanical Engineering 36, 1, 13, 2012.

[29] J. Novak, Molecular dynamics simulation of aluminium melting. Materials and Geoenvironment 63, 1, 9-18, 2016.

[30] A. V. Karavaev, V. V. Dremov and T. A. Pravishkina. Precise calculation of melting curves by molecular dynamics. Computational Materials Science 124, 335-343, 2016.

[31] C. S. Hsu, and A. Rahman. Crystal nucleation and growth in liquid rubidium. The Journal of Chemical Physics 70, 11, 5234-5240, 1979.

[32] E. V. Levchenko, A. V. Evteev, I. V. Belova, and G. E. Murch. Molecular dynamics determination of the time–temperature–transformation diagram for crystallization of an undercooled liquid Ni 50 Al 50 alloy. Acta Materialia 59, 16, 6412-6419, 2011.

[33] Y. Shibuta, S. Sakane, T. Takaki and M. Ohno. Submicrometer-scale molecular dynamics simulation of nucleation and solidification from undercooled melt: Linkage between empirical interpretation and atomistic nature. Acta Materialia 105, 328-337, 2016.

[34] Y. J. Lü, M. Chen, H. Yang, and D. Q. Yu. Nucleation of Ni–Fe alloy near the spinodal. Acta Materialia 56, 15, 4022-4027, 2008.

[35] B. Mantisi, Generation of polycrystalline material at the atomic scale. Computational Materials Science 118, 245-250, 2016.

[36] S. Plimpton, Fast parallel algorithms for short-range molecular dynamics,J. Comput. Phys. 117, 1, 1-19, 1995.

[37] W. Humphrey, A. Dalke, K. Schulten, VMD: visual molecular dynamics, J. Mol.Graph. 14 (1), 33-38, 1996.

[38] *A. Stukowski, Visualization and analysis of atomistic simulation data with OVITO – the Open Visualization Tool, Modelling Simul. Mater. Sci. Eng. 18, 015012, 2010.*

[39] M.I. Mendelev, M.J. Kramer, C.A. Becker, and M. Asta, Analysis of semi-empirical interatomic potentials appropriate for simulation of crystalline and liquid Al and Cu, Phil. Mag. 88, 1723-1750, 2008.

[40] L. Verlet, Computer " experiments" on classical fluids. I. Thermodynamical properties of Lennard-Jones molecules. Physical review 159, 1, 98, 1967.

[41] B. G. Levine, J. E. Stone, A. Kohlmeyer, Fast analysis of molecular dynamicstrajectories with graphics processing unit's Radial distribution function histogramming, J. Comput. Phys. 230 (9), 3556-3569, 2011.

[42] Y. Waseda, The structure of non-crystalline materials: liquids and amorphous solids. (1980).

[43] P. J. Steinhardt, D. R. Nelson, and M. Ronchetti. Bond-orientational order in liquids and glasses. Physical Review B 28, 2, 784, 1983.

[44] P. J. Steinhardt, D. R. Nelson, and M. Ronchetti. Icosahedral bond orientational order in supercooled liquids. Physical Review Letters 47, 18, 1297, 1981.

[45] Y. Wang, S. Teitel, and Christoph Dellago. Melting of icosahedral gold nanoclusters from molecular dynamics simulations. The Journal of chemical physics 122, 21, 214722, 2005.

[46] W. Lechner, and Christoph Dellago. Accurate determination of crystal structures based on averaged local bond order parameters. The Journal of chemical physics 129, 11, 114707, 2008.

[47] B. Cichocki, and K. Hinsen. Dynamic computer simulation of concentrated hard sphere suspensions: I. Simulation technique and mean square displacement data. Physica A: Statistical Mechanics and its Applications166, 3, 473-491, 1990.

[48] M. P. Allen, and D. J. Tildesley. Computer simulation of liquids. Oxford university press, (1989).

[49] D. Frenkel, and B. Smit. Understanding molecular simulations: from algorithms to applications. Academic, San Diego (1996).

[50] A. Stukowski, V. V. Bulatov, and A. Arsenlis. Automated identification and indexing of dislocations in crystal interfaces. Modelling and Simulation in Materials Science and Engineering 20, 8, 085007, 2012.

[51] A. Stukowski, Computational analysis methods in atomistic modeling of crystals. Jom 66, 3, 399-407, 2014.

[52] A. Stukowski, and K. Albe. Extracting dislocations and non-dislocation crystal defects from atomistic simulation data. Modelling and Simulation in Materials Science and Engineering 18, 8, 085001, 2010.

[53] F. Kargl, H. Weis, T. Unruh, and A. Meyer. Self diffusion in liquid aluminium. In Journal of Physics: Conference Series 340, 012077, 2012.

[54] V. S.. Krasnikov, A. E. Mayer, and V. V. Pogorelko. Prediction of the shear strength of aluminum with θ phase inclusions based on precipitate statistics, dislocation and molecular dynamics. International Journal of Plasticity 128, 102672, 2020.

[55] N. Gunkelmann, E. M. Bringa, and Y. Rosandi. Molecular dynamics simulations of aluminum foams under tension: influence of oxidation. The Journal of Physical Chemistry C 122, 45, 26243-26250, 2018.

[56] Z. Li, Y. Gao, S. Zhan, H. Fang, Z. Zhang. Molecular dynamics study on temperature and strain rate dependences of mechanical properties of single crystal Al under uniaxial loading. AIP Advances 10, 7, 075321, 2020.